HHS Public Access

Author manuscript

J Neurochem. Author manuscript; available in PMC 2017 September 01.

Published in final edited form as:

J Neurochem. 2016 September ; 138(5): 746–757. doi:10.1111/jnc.13706.

Dopaminergic neuron-specific deletion of p53 gene is neuroprotective in an experimental Parkinson's disease model

Xin Qi, PhD[2], **Brandon Davis, BA**[1], **Yung-Hsiao Chiang**[3], **Emily Filichia, BA**[1], **Austin Barnett, BA**[1], **Nigel H. Greig, PhD**[4], **Barry Hoffer, MD PhD**[1], and **Yu Luo, PhD**[1]

[1]Department of Neurological Surgery, Case Western Reserve University, Cleveland, USA

[2]Department of Physiology & Biophysics, Case Western Reserve University, Cleveland, USA

[3] Division of Neurosurgery, Department of Surgery, College of Medicine, Taipei Medical University, Taipei

[4]Drug Design & Development Section, Translational Gerontology Branch, Intramural Research Program, National Institute of Aging, Baltimore, USA

Abstract

p53, a stress response gene, is involved in diverse cell death pathways and its activation has been implicated in the pathogenesis of Parkinson's disease (PD). However, whether the neuronal p53 protein plays a direct role in regulating dopaminergic (DA) neuronal cell death is unknown. In this study, in contrast to the global inhibition of p53 function by pharmacological inhibitors and in traditional p53 knock-out (KO) mice, we examined the effect of DA specific p53 gene deletion in DAT-p53KO mice. These DAT-p53KO mice did not exhibit apparent changes in the general structure and neuronal density of DA neurons during late development and in aging. However, in DA-p53KO mice treated with the neurotoxin MPTP (1-methyl-4-phenyl-1,2,3,6-tetrahydropyridine), we found that the induction of Bax and PUMA mRNA and protein levels by MPTP were diminished in both striatum and substantia nigra (SN) of these mice. Notably, deletion of the p53 gene in DA neurons significantly reduced dopaminergic neuronal loss in SN, dopaminergic neuronal terminal loss at striatum and, additionally, decreased motor deficits in mice challenged with MPTP. In contrast, there was no difference in astrogliosis between WT and DAT-p53KO mice in response to MPTP treatment. These findings demonstrate a specific contribution of p53 activation in DA neuronal cell death by MPTP challenge. Our results further support the role of programmed cell death mediated by p53 in this animal model of PD and identify Bax, BAD and PUMA genes as downstream targets of p53 in modulating DA neuronal death in the *in vivo* MPTP-induced PD model.

Graphical abstract

Correspondence to Yu Luo, PhD, Department of Neurological Surgery, Case Western Reserve University, 2109 Adelbert Rd, Cleveland, OH, USA. **yxl710@case.edu**, Phone: 01-216-368-4169.

ARRIVE guidelines have been followed:

Yes

=> if No, skip complete sentence

=> if Yes, insert “All experiments were conducted in compliance with the ARRIVE guidelines.”

The authors declare no competing financial interests.

We deleted p53 gene in dopaminergic neurons in late developmental stages and found that DA specific p53 deletion is protective in acute MPTP animal model possibly through blocking MPTP-induced BAX and PUMA upregulation. Astrocyte activation measured by GFAP positive cells and GFAP gene upregulation in the striatum shows no difference between wt and DA-p53 ko mice.

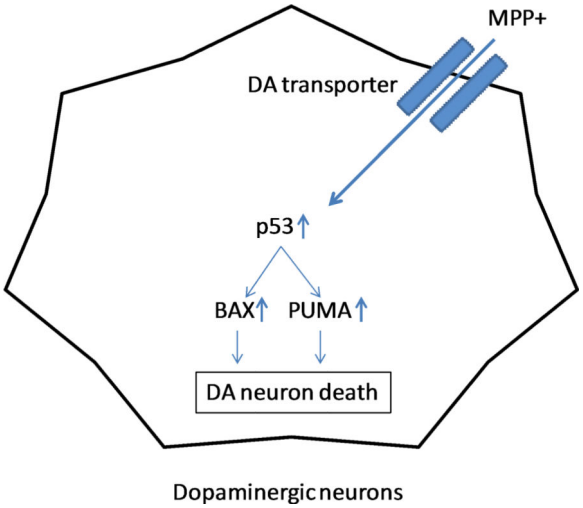

Introduction

Parkinson's disease (PD) is a neurodegenerative disorder characterized by a progressive degeneration of dopaminergic neurons in the substantia nigra pars compacta region of the midbrain. Despite decades of research, the mechanism underlying selective neuronal degeneration in PD remains elusive. p53 is a well-known stress response gene implicated in programmed cell death in various diseased models (Culmsee & Mattson 2005). Accumulating evidence indicates a mechanistic link between p53 and the pathogenesis of PD (Alves da Costa & Checler 2011). Post-mortem studies have demonstrated an increase in p53 expression and its target gene, Bax in post mortem tissues in PD patients (de la Monte *et al.* 1998, Mogi *et al.* 2007, Hartmann *et al.* 2001). In neurotoxicant- induced PD models (Blesa *et al.* 2012), it has been shown that loss or compromised p53 function is protective for dopaminergic neurons in toxin exposure models such as MPTP (1-methyl-4-phenyl-1,2,3,6-tetrahydropyridine) (Trimmer *et al.* 1996, Perier *et al.* 2007) and methamphetamine (Hirata & Cadet 1997). Interestingly, recent discoveries suggest that p53 is also implicated in familial PD through parkin-mediated transcriptional regulation of p53 (da Costa *et al.* 2009) and is involved in the regulation of DJ-1 mRNA and protein expression by parkin (Duplan *et al.* 2013). Taken together these findings suggest that p53 might be a “missing link” between genetic and sporadic Parkinsonism (Alves da Costa & Checler 2011).

The fact that the induction of p53-dependent cell death pathway exists in both human PD and experimental PD animal models raises the possibility that inhibition of p53 may serve as a therapeutic strategy to reduce neurodegenerative processes in PD. However, the specificity and the efficacy of delivery of p53 inhibitors into neurons within the CNS is difficult to control, and traditional knockouts (KOs) of p53 can introduce confounding factors into the interpretation of the results (Donehower 1996). In addition, development of malignancies in

traditional p53 KO mice can introduce problems with the overall health of the animal as well as alterations in metabolism (Donehower 1996, Liang *et al.* 2013, Yokoyama *et al.* 2014). Since p53 is involved in cell cycle regulation, disruption of its function early in development could also lead to abnormalities in developmental processes (Armstrong *et al.* 1995, Kawamata & Ochiya 2012). Premature death in animals would make it impossible to study the role of p53 in the normal aging process. Therefore, to clearly elucidate the role of p53-regulated cell death in the development and survival of dopaminergic neurons during normal ageing, toxic/stress conditions and during grafting processes, cell type specific deletion of p53 function is needed.

Our group has previously developed a cre knock-in animal model, in which a cre recombinase gene is specifically inserted in the dopamine transporter (DAT) locus, providing dopaminergic neuron specific cre expression with minimal interference with endogenous DAT gene expression (Backman *et al.* 2006). Utilizing this cre-loxP dopaminergic-neuron specific deletion system, we previously reported that developmental apoptosis is important in determining the ultimate numbers and anatomy of the nigro-striatal dopamine (DA) projection and that the Phosphatase and tensin homolog (PTEN) gene plays an essential role in this process (Zhang *et al.* 2012). In this study, we utilized the same system to examine the role of the p53 gene in the naturally occurring apoptosis in midbrain dopaminergic neurons during late embryonic development, normal aging during adulthood, and in neurotoxin-induced dopaminergic neuronal death. In the present communication, we document the role of DA neuronal p53 in the loss of the nigrostriatal DA system induced by MPTP. Our results further support the role of programmed cell death mediated by p53 in this animal model of PD and indicate that the Bax and p53 upregulated modulator of apoptosis (PUMA) genes are downstream targets of p53 in modulating DA neuronal death in this *in vivo* MPTP-induced PD model.

Materials and methods

Animals and treatment

All animal protocols were conducted under National Institutes Health (NIH) Guidelines using the NIH handbook *Animals in Research* and were approved by the Institutional Animal Care and Use Committee of Case Western Reserve University. The mice were housed in the animal facility of Case Western Reserve University on a 12-h light/dark diurnal cycle. Food was provided ad libitum. For the conditional inactivation of *p53* in dopaminergic neurons, a transgenic line, *Slc6a3*^{Cre} was used in which Cre recombinase is driven by the DA transporter promoter starting at about embryonic day 16 (Backman et al. 2006). To minimize interference with gene function by preservation of both alleles, Cre recombinase expression was driven from the 3′ untranslated region (3′ UTR) of the endogenous DAT gene by means of an IRES sequence (Backman et al. 2006). Dopaminergic neuronal specific p53 knockout (KO) mice (DATcreTRP53 KO, Fig 1A) were generated by crossing TRP53$^{loxP/loxP}$ mice (Jonkers *et al.* 2001) with *Slc6a3*^{Cre} knock-in mice to obtain DATcre(wt/+)/TRP53 $^{loxP/loxP}$ (DAT p53 KO mice) or DATcre (+/−)/TRP53$^{wt/wt}$ (DAT p53 wildtype (WT)) mice. The DAT-IRES-Cre gene was genotyped using primers (5′ TGG CTG TTG GTG TAA AGT GG -3′; 5′ GGA CAG GGA CAT GGT TGA CT -3′; 5′ CCA AAA

GAC GGC AAT ATG GT -3′). TRP53 floxed alles were genotyped by the primer set (5′ CAC AAA AAC AGG TTA AAC CCA G-3′; 5′ AGC ACA TAG GAG GCA GAG AC-3′). Olfactory bulb, hippocampus, cortex, ventral tegmental area (VTA), cerebellum, striatum and substantia nigra tissue were punched out using the Paxinos atlas, as we have previously described (Filichia *et al.* 2015), and DNA was extracted for PCR analysis. Deletion of the exon 1-10 of the p53 gene results in amplification of a ΔloxP band, which is amplified by a set of primers flanking the 5' of exon 1 and 3' of exon 10 (Fig 1B).

Because different strains of mice have differential vulnerability to MPTP toxicity, all mice strains used here were maintained in a C57BL/6 genetic background. Nine to ten week-old DAT p53 KO or DAT p53 WT male mice received four i.p. injections of MPTP. -HCl in one day with 2 hour intervals between each injection (15 mg/kg/injection, free base, Sigma-Aldrich, St. Louis, MO) and were euthanized at the indicated time points after the last MPTP injection. Saline was injected as a control in both WT and KO mice.

Experimental timeline for experiments

For the normal aging study, 3 month and 20 month old male mice (n=11-12 each group) were subjected to spontaneous locomotion tests. After the behavioral tests, animals were perfused for dopaminergic neuronal counts and striatal tyrosine hydroxylase (TH) fiber density quantification (n= 6-8 each group).

For MPTP experiments, male adult (9-10 week old) DATcreTRP53 KO (n=12) and WT (n=12) mice were initially subjected to rotarod training and testing before MPTP administration. 1 week after MPTP injection (4X 15mg/kg i.p with 2 hour intervals), animals were tested for rotarod performance again. At 2 weeks after MPTP injection, WT and KO mice were perfused with 4% paraformaldehyde (PFA) and the brains were subjected to immunostaining for the nigrostriatal pathway (n=9 each group for MPTP treated mice). Control WT and KO mice (same age, n=5 each group) were subjected to saline injections and harvested at the same time for immunostaining. Another set of WT and KO mice were euthanized 48 hours after saline or MPTP injection and brain tissues (ventral midbrain and striatum) were harvested for gene expression analysis (RT-PCR, n=7-8 each group), and protein expression analysis (Western blotting, n=4 each group) or were perfused for immunostaining (n= 4 each group).

Immunostaining

Animals were anesthetized and perfused transcardially with saline followed by 4% PFA in phosphate buffer (PB; 0.1 M; pH 7.2) at different ages or after different treatments. The brains were removed, dissected, postfixed in PFA for 16 hours, and transferred to 20% and 30% sucrose in 0.1 M PB sequentially. Serial sections of the entire brain were sliced at 30 or 40 μm thickness in a cryostat. One series from every 4th section was stained for each antibody used. In order to control for staining variability, specimens from all experimental groups were included in every batch and reacted together in a net well tray under the same conditions as described in our previous study (Luo *et al.* 2010). Sections were rinsed in 0.1M PB, and blocked with 4% bovine serum albumin (BSA) and 0.3% Triton x-100 in 0.1M PB. Sections were then incubated in a primary antibody solution of rabbit anti-TH (1:1000,

Chemicon, Temecula, CA) diluted in 4% BSA and 0.3% Triton x-100 in 0.1M PB for 24 hours at 4°C. Sections were rinsed in 0.1M PB and incubated in biotinylated goat anti-rabbit IgG for TH or anti-mouse IgG for GFAP in the buffer (1:200; Vector Laboratories, Burlingame CA) for 1 hour, followed by incubation for 1 hour with avidin-biotin-horseradish peroxidase complex. Staining was developed with 2,3' diaminobenzidine tetrahydrochloride (0.5 mg/mL in 50 mM Tris-HCl buffer 7.4). Control sections were incubated without primary antibody. Sections were mounted on slides, and cover slipped. Histological images were acquired using an Infinity3 camera and NIKON 80i microscope. TH immunoreactivity in striatum was visualized with the use of a Nikon super-coolscan 9000 scanner. The optical density of TH immunoreactivity in striatum was analyzed using Scion Image (ver 4.02) and averaged from 3 sections with a visualized anterior commissure (AP: +0.26 mm, +0.14 mm, +0.02 mm to bregma), as previously described (Luo et al. 2010). Observers who were blinded to the experimental groups performed all immunohistochemical measurements. Slight variations in background staining were corrected by subtracting background density of cortical regions from striatal density measurements.

For analysis of activated astrocytes, brain sections were stained with mouse anti-GFAP (1:500, Sigma Aldrich) followed by incubation with diluted secondary antibody prepared with blocking solution (goat anti-mouse 568, 1:1000; Life Technologies). The slides were then washed with 0.1% Triton-X100 in TBS (tris buffered saline) and coverslipped. Images were acquired using an Olympus fluorescent microscope. Omission of the primary or secondary antibodies resulted in no staining and served as negative controls. GFAP immunoreactivity in the striatal area was quantified using Nikon NIS-Elements software and was averaged from 3 sections for each animal, as previously described (Jin *et al.* 2015).

Stereologic Analysis

Unbiased stereological counts of TH-positive (TH+) neurons within the substantia nigra pas compacta (SNpc) were performed using stereological principles and analyzed with StereoInvestigator software (Microbrightfield, Williston, VT), as previously described (Luo et al. 2010). Optical fractionator sampling (West & Gundersen 1990) was carried out on a Leica DM5000B microscope (Leica Microsystems, Bannockburn, IL) equipped with a motorized stage and Lucivid attachment (40X objective). Midbrain dopaminergic groups were outlined on the basis of TH immunolabelling, with reference to a coronal atlas of the mouse brain (Franklin and Paxinos, (Franklin KBJ 1997)). For each tissue section analyzed, section thickness was assessed in each sampling site and guard zones of 2.5μm were used at the top and bottom of each section. Pilot studies were used to determine suitable counting frame and sampling grid dimensions prior to counting. The following stereologic parameters were used in the final study: grid size, (X) 220 μm, (Y) 166 μm; counting frame, (X) 68.2 μm, (Y) 75 μm, depth was 20 μm. Gundersen coefficients of error for m=1 were all less than 0.10. Stereologic estimations were performed with the same parameters in the SNpc of WT or DATcreTRP53 KO mice at different ages, or treated with saline or MPTP.

Quantitative reverse transcription-PCR (qRT-PCR)

Tissues were harvested for qRT-PCR analysis at 48 hours after the last MPTP or saline injection. Mice were euthanized and the brains were immediately harvested and chilled on

ice. The striatum or ventral midbrain was punched out using the Paxinos atlas and total RNA was extracted following the instructions from the manufacturer (RNAqueous, Ambion). Total RNA (0.7 μg) was treated with RQ-1 Rnase-free Dnase I and reverse transcribed into cDNA using random hexamers by Superscript III reverse transcriptase (Life Sciences). cDNA levels for HPRT1 (hypoxanthine phosphoribosyltransferase 1), Hmbs (hydroxymethylbilane synthase) and various target genes were determined using specific universal probe Library primer probe sets (Roche) by quantitative RT-PCR using a Roche Light Cycler II 480. A relative expression level was calculated using the delta delta Ct method compared to Hmbs as a reference gene, with a N=7-8 for each group. Primers and FAM-labeled probes used in the quantitative RT-PCR for each gene are listed in Table 1.

Western-blot analysis—Brain tissue of substantia nigra and striatum were harvested and lysed in the following lysis buffer (10 mM HEPES-NaOH, pH 7.5, 150 mM NaCl, 1 mM EGTA, 1 % Triton X-100, 1:300 protease inhibitor cocktail, 1:300 phosphatase inhibitor cocktail). After 20 minutes of incubation on ice, homogenates were spun at 14,000 rpm for 20 minutes at 4°C. The supernatants correspond to the total cell lysates. Protein concentrations were determined by Bradford assay. Thirty μg of proteins were resuspended in Laemmli buffer, loaded on SDS-PAGE and transferred onto nitrocellulose membranes. Membranes were probed with the indicated antibodies followed by visualization by ECL, and then were quantitated using NIH ImageJ software. The antibodies used in this study include Bax (1:1000, Proteintech Group Inc), PUMA (1:200, Proteintech Group Inc) and Actin (1:10000, Sigma).

Behavioral tests

Open field locomotion—The rotarod and open field tests have been shown to provide reliable measures of motor function for MPTP-challenged mice (Hutter-Saunders *et al.* 2012) and hence were used here to evaluate the motor deficits in WT and KO mice administered MPTP. Locomotion function was measured in young (3 months) and old (20 months) WT and DATcreTRP53 KO mice as described previously. In synopsis, spontaneous locomotor functions were examined using automated infra-red locomotor activity chambers, as previously described (Luo *et al.* 2009). Locomotor function was assessed during a 120 min trial in an open field crossed by a grid of photobeams (VersaMax system, AccuScan Instruments). Counts were taken of the number of photobeams broken during the trial at 5 min intervals, with separate measures for total horizontal and vertical activity, and total movement time. Total horizontal and vertical activities correspond to the total number of beam interruptions that occurred in the horizontal and vertical sensors, respectively, during a given sample period.

Rotarod—The rotarod is specifically designed for making automated measurements of neurological deficits in rodents and is one of the most commonly used tests of motor function in mice (Luft & Buitrago 2005, Yin *et al.* 2009) including detection of deficits after MPTP treatment (Hutter-Saunders et al. 2012, Lee *et al.* 2013). In this study, motor coordination and balance were evaluated using a fixed speed rotarod test. A rotarod apparatus (Accuscan Instruments) with a 30-mm-diameter rod was set to rotate at 10 rpm revolutions per minute (rpm) over 300 sec. Mice, both WT (n = 12) and DA-p53 KO (n =

12), were first trained for 6 trials at 2.5 rpm, 5 rpm, 7.5 rpm and 10 rpm during 2 days. Rest between trials was for 30 sec. After the 2 day training, mice were placed on the rod apparatus rotating at 10 rpm, and the latency to fall was recorded before MPTP injection. At 1 week after MPTP injection, mice were again tested under the same conditions. The time each mouse stayed on the rod at 10 rpm was calculated as a percentage of the time it stayed on the rod before MPTP injection to account for individual variations.

Statistics—Statistical analysis was performed using Student's *t* test, and one- or two-way analysis of variance (ANOVA), as appropriate, with Newman–Keuls post hoc tests. A *p* value of equal or less than 0.05 was considered significant.

Results

Characterization of mice with specific deletion of p53 in DAT-expressing DA neurons

Our strategy for deletion of p53 in DAT expressing neurons is shown in Fig 1A. To achieve dopaminergic-specific p53 deletion, we used the *Slc6a3*^{Cre} line, a cre knock-in animal model, in which a cre recombinase gene is specifically inserted in the DAT locus of the 3′ UTR of the endogenous DAT gene following an IRES (internal ribosome entry site sequence). This provides dopaminergic neuron-specific cre expression with minimum interference with endogenous DAT gene expression (Backman et al. 2006). In this mouse line, Cre recombinase is driven by the DA transporter promoter starting at about embryonic day 16. To determine the specific deletion of the mTRP53 gene in DAT-expressing dopaminergic neurons, primers specific for the recombined DNA sequence (ΔloxP) were used to amplify the recombined TRP53 allele. As expected, only brain tissues obtained from the olfactory bulb, ventral tegmental area (VTA) and substantia nigra (SN) contained ΔloxP, thereby confirming the deletion of the p53 gene in these brain areas (Fig 1B). In contrast, the cortex, hippocampus, striatum and cerebellum were found to be negative for ΔloxP, indicating lack of p53 gene deletion in these areas in our DAT-p53 KO mice. No recombination was seen in WT mice.

In order to determine whether or not p53 ablation in DA systems offers neuroprotection after MPTP treatment, it was first necessary to determine if there are differences in the nigrostriatal system in the WT vs. KO animals. The TRP53^{DATCre} KO animals were born at expected Mendelian frequencies and showed normal viability. The body weights of adult (3 month old) KO and WT mice were not significantly different (WT male=25.9±0.4g (n=30), KO male= 26.3±0.3g (n=37); p=0.45, Student's t-test). Loss of the p53 gene in DAT positive- dopaminergic neurons did not lead to an abnormal development of ventral midbrain, as demonstrated by the normal structure and number of midbrain dopaminergic neurons within the SN and TH positive projections in striatum in DAT-p53 KO mice at 3 month of age (Fig 2 A). As shown in Fig 2A, TH immunocytochemistry evaluated at three different levels within the SN showed no overt morphological differences at either 3 months or 20 months of age. Moreover, unbiased stereological counts of SN DA neuron numbers (Fig 2B) showed no difference in total TH positive neurons within SN in WT and DAT-p53 KO mice at 3 or 20 months of age (Two-way ANOVA, genotype: $F_{1, 21} = 0.275$, p=0.606; age: $F_{1, 21} = 1.681$, p=0.211, n=5-6 per group). In addition, striatal DA fiber densities (Fig

2C) were similar in WT and DAT-p53 KO mice (Fig 2C) at both ages (Two-way ANOVA, genotype: $F_{1, 23} = 0.123$, p=0.730; age: $F_{1, 23} = 0.433$, p=0.518, n=6-8 per group). Basal locomotion tests performed in automated behavioral chambers did not reveal any difference between the WT and DAT-p53 KO mice at both age groups for total horizontal activity (Fig 2D, Two-way ANOVA, genotype: $F_{1, 42} = 2.791$, p=0.103; age: $F_{1, 42} = 2.815$, p=0.101, n=10-12 per group). Vertical movement was reduced in old vs. young animals but again there were no differences between WT and KO mice at either age (Fig 2E, Two-way ANOVA, genotype: $F_{1, 42} = 0.573$, p=0.454; age: $F_{1, 42} = 37.603$, p<0.001, n=10-12 per group).

Deletion of the p53 gene results in reduced toxicity in the nigrostriatal system after MPTP

Since the baseline nigrostriatal parameters were similar between the WT and KO mice, we next tested the responses of these mice to acute MPTP administration. Two weeks after the last MPTP injection using an acute MPTP injection regimen (4X 15 mg/kg i.p with 2 hour intervals), the dopaminergic system was evaluated by TH immunostaining and behavioral analyses. TH staining of cell bodies in the SN (Figs 3A, C) and fiber densities in striatum (Figs 3B, D) indicated that dopaminergic neuronal specific p53 deletion significantly reduced MPTP toxicity in the nigrostriatal DA system. Unbiased stereological counts showed that MPTP injection significantly decreases the TH positive neurons in SN (Two-way ANOVA, treatment: $F_{1, 27} = 53.595$, p<0.001) and DAT-p53 ko showed a significant protection of SN DA neurons (Two-way ANOVA, genotype: $F_{1, 27} = 7.066$, p=0.014, n=5 for saline treated groups and n=9 for MPTP treated groups). There is a significant interaction between the treatment and genotype (Two-way ANOVA, genotype x treatment, $F_{1, 27} = 4.738$, p = 0.04). Saline injected WT and DAT-p53 mice have no differences in SN DA neuronal counts (p=0.767 post hoc Student-Newman-Keuls Method) while MPTP-treated DAT-p53 KO mice had significantly more TH positive neurons compared to WT MPTP treated mice (Fig 3C, p<0.001, post hoc Student-Newman-Keuls Method, n=9 per group). Similarly, quantification of TH positive fiber density in striatum showed higher optical densities in MPTP-treated DAT-p53 KO mice than in MPTP-treated WT mice (Fig 3D, p<0.001, ANOVA, post hoc Student-Newman-Keuls Method, n=9 per group). This was also manifested behaviorally, as vertical movement (rearing) was significantly higher in MPTP-challenged KO mice when compared to MPTP-challenged WT mice (Fig 3E, p=0.01, ANOVA, n=12 per group). Similarly, motor coordination was significantly better in MPTP-challenged KO mice than that in MPTP-challenged WT animals, measured using the rotarod test. MPTP administration resulted in reduction in the time that WT mice proved capable of remaining on the rotorod (64.8% of pretreatment latency, Fig 3F) but did not affect the time that KO mice stayed on the rotarod (99.79% of pretreatment latency, Fig 3F, p<0.009, WT vs. KO, Student's t-test, n=10-12 per group).

Dopaminergic neuronal specific deletion of p53 suppresses BAX, BAD and PUMA upregulation produced by MPTP exposure-

We next examined changes in gene expression in the nigrostriatal system after MPTP challenge to evaluate the impact of p53 deletion. MPTP induced p53 upregulation in WT mice (Fig 4A, treatment: $F_{1, 29} = 63.367$, p < 0.001, TWO WAY ANOVA and p<0.001 saline vs. MPTP in WT, post hoc Student-Newman-Keuls Method, n=7-8 per group) but not in

DA-p53 KO mice at 48 hours after the last MPTP injection (Fig 4A, genotype: $F_{1, 29}$ = 6.689, p =0.016, TWO WAY ANOVA and p=0.001 post hoc Student-Newman-Keuls Method, WT MPTP vs. KO MPTP, n=7-8 per group). MPTP challenge also induced BAX, BAD and PUMA gene upregulation in WT mice (Fig 4B, C and D, saline vs. MPTP in WT for BAX, BAD and PUMA p<0.001, TWO WAY ANOVA, post hoc Student-Newman-Keuls Method, n=7 per group). DA-p53 KO mice had diminished upregulation of BAX, BAD and PUMA genes compared to WT mice (Fig 4B, C and D, WT MPTP vs. KO MPTP, for BAX and PUMA, p<0.001 and BAD p=0.048, TWO WAY ANOVA, post hoc Student-Newman-Keuls Method, n=8 per group). MPTP also resulted in down regulation of BCLX (Fig 4E) and upregulation of BAK genes (Fig 4F, saline vs. MPTP in WT for BCLX and BAK p<0.001, TWO WAY ANOVA, post hoc Student-Newman-Keuls Method, n=7 per group), neither of which are transcriptional targets of the p53 gene. Dopaminergic specific p53 deletion in DA-p53 KO mice did not affect BCLX gene downregulation and BAK gene upregulation induced by MPTP (Fig 4E, F WT MPTP vs. KO MPTP, for BCLX p=0.106 and BAK p=0.084, TWO WAY ANOVA, post hoc Student-Newman-Keuls Method, n=8 per group). Changes in Bax and PUMA gene expression were also confirmed at the protein levels (Fig 5, saline vs. MPTP in WT for BAX p=0.003 for striatum/ p=0.006 for SN and PUMA p=0.01 for striatum/ p=0.008 for SN, TWO WAY ANOVA, post hoc Student-Newman-Keuls Method, n=4 per group). Dopaminergic neuronal specific p53 deletion in mice inhibited MPTP-induced Bax and PUMA protein upregulation at 48 hours after the last MPTP injection (Fig 5A and 5B, WT MPTP vs. KO MPTP, for BAX p=0.004 for striatum/ p=0.008 for SN and PUMA, p=0.006 for striatum/ p= 0.007 for SN, TWO WAY ANOVA, post hoc Student-Newman-Keuls Method, n=4 per group).

Dopaminergic neuronal specific deletion of p53 does not affect astrogliosis in mice challenged with MPTP

Astrocyte activation has been reported to be a key feature in the MPTP-induced Parkinsonism model (Langston *et al.* 1999, Vila *et al.* 2001a, Yokoyama *et al.* 2011). We thus examined whether astrogliosis is influenced in DAT-p53 KO mice. Although DAT-p53 KO mice showed protection of the DA system in this acute MPTP model, the extent of astrogliosis in DAT-p53 KO mice was similar to that in WT mice (Fig 6 A-F). As shown in Figure 6, MPTP administration elicited significant astrocytic activation, indicated by GFAP gene expression in striatum (Fig 6G, saline vs MPTP, $F_{1,29}$= 315.359, p<0.001, TWO WAY ANOVA, n=7-8 per group) and SN (Fig 6H, saline vs MPTP, $F_{1,29}$= 14.077, p<0.001, TWO WAY ANOVA, n=7-8 per group). There was no significant difference between WT and KO animals (Fig 6G WT vs KO, $F_{1,29}$= 2.667, p=0.115, TWO WAY ANOVA, n=7-8 per group for STR and Fig 6H WT vs KO, $F_{1,29}$= 0.271, p=0.607, TWO WAY ANOVA, n=7-8 per group). Striatal GFAP immunostaining (Fig 6A-H) also showed robust activation of astrocytes in both MPTP-injected WT and KO mice, as demonstrated by similar immunoreactivity of GFAP in both groups (Fig 6I, p=0.836 WT vs. KO, Student's t-test, n=4 mice for each group). This suggests that astrogliosis might not be sufficient to lead to neuronal death in the absence of the p53 gene in dopaminergic neurons.

Discussion

Programmed cell death by apoptosis is an essential component of neural development whereby the eventual neuronal population is determined by the establishment of proper neuron:target cell connections. The p53 gene has been demonstrated to be essential for natural neuronal apoptosis in the CNS. However, the role of p53 in the developmental apoptosis in midbrain DA neurons is unknown. For DA neurons in mouse ventral midbrain, two peaks of apoptosis occur, at birth and around 2 weeks of postnatal age (Jackson-Lewis *et al.* 2000, Linden 1994, Hattori & McGeer 1973). We have previously reported that developmental apoptosis is important in determining the ultimate numbers and anatomy of nigro-strital DA projection and that the PTEN gene plays an essential role in this process (Diaz-Ruiz *et al.* 2009). Therefore, pathological apoptosis due to disregulated p53 expression/function could potentially lead to a reduced number of DA neurons, which might result in a loss of DA function during aging. Utilizing a dopaminergic-neuron specific p53 deletion animal model in this study, we examined, for the first time, the role of the p53 gene in naturally occurring apoptosis in midbrain dopaminergic neurons during the late developmental stage and in aging. Loss of the p53 gene in DAT positive- dopaminergic neurons did not lead to an abnormal development of the ventral midbrain, as demonstrated by the normal structure and number of midbrain dopaminergic neurons in SN, and TH positive projections in striatum in DAT-p53 KO mice at 3 months of age (Fig. 2). Therefore, our data suggest that unlike the PTEN gene, the p53 gene might not be critical for the apoptotic processes that eliminate excess neurons during postnatal development (Kim & Sun 2011).

We also examined the ventral midbrain nigrastrial pathway in aged WT and KO mice. Our results show that at 3 and 20 months, the number of dopaminergic cells remained almost constant, consistent with previous reports (Schumm *et al.* 2012). Moreover, DA-p53 KO mice showed no difference, compared to WT littermates, in regards to dopaminergic neuron number and striatal TH-positive fiber density. Horizontal activity remained constant across 3 and 20 month old WT and DA-p53 KO mice. There was a significant decrease in vertical activity in 20 month old mice, but no difference was observed between WT and DA-p53 KO mice. Thus, we conclude that dopaminergic neuronal specific deletion of the p53 gene does not cause any apparent changes in the general structure or neuronal density of DA neurons during perinatal development and the normal process of aging. This model thus enables us to examine the role of the p53 gene in dopaminergic neuronal cell death in PD animal models, such as the MPTP neurotoxin model, without potential confounding factors.

We have previously reported that in a stroke animal model, neuronal p53 expression directly regulates neuronal cell death (Filichia et al. 2015). Whether p53 function determines the outcome of dopaminergic function in PD animal models by either directly regulating the cell death of neurons or through indirect modulation of the microenvironment in the dopaminergic system remains to be analyzed. Our data does, however, show that DA specific p53 deletion diminishes MPTP induced dopaminergic neuronal loss in SN and dopaminergic neuronal terminal loss in striatum. Dopaminergic neuronal specific p53 deletion also reduced certain behavioral deficits caused by MPTP administration, including loss of motor coordination analyzed by rotarod tests. MPTP-treated DA-p53 KO mice also showed greater

vertical activity but not overall horizontal activity compared to MPTP-treated WT mice. Therefore, our data support the notion that DA neuronal specific p53 function is directly involved in the process of dopaminergic neuronal cell death in this PD animal model.

p53 directly activates the proapoptotic Bcl-2 protein BAX to permeabilize mitochondria, which results in the release of mitochondrial factors, such as cytochrome c, that signal apoptotic cell death (Chipuk *et al.* 2004). Increased BAX levels have been found in the MPTP-induced PD mouse model (Vila *et al.* 2001b, Perier et al. 2007) and in a subset of dopaminergic neurons in PD patients (Tatton 2000, Hartmann et al. 2001). Ablation of BAX in mice reduced dopaminergic neuronal degeneration induced by MPTP-treatment (Vila et al. 2001b). In our DA specific p53 KO mice, we found that MPTP-induced p53 upregulation is diminished in DA-p53 KO mice, supporting a midbrain dopaminergic neuron (DAN)-specific p53 response. Our data further showed that MPTP-induced BAX up-regulation is dependent on dopaminergic p53 function as evidenced by the fact that selective depletion of p53 in DA neurons abolished BAX induction by MPTP treatment. In addition, we found that BCLX was down-regulated in MPTP injected mice, which is consistent with the findings from qRT-PCR validated microarray studies (Miller *et al.* 2005, Miller *et al.* 2004), whereas the BAK gene was up-regulated by MPTP challenge. However, there was no difference in the expression of these genes between WT and DAT-p53 KO mice, confirming that p53 does not directly regulate BCLX and BAK transcription. We also identified BAD and PUMA as p53-dependent regulators of dopaminergic neuronal cell death in our animal model. PUMA levels were reported to be not affected in a previous study using a subacute MPTP model (Perier et al. 2007) but was recently implicated in an in vitro cell model using MPP+ (Bernstein & O'Malley 2013). In our acute MPTP model, we found that PUMA gene and protein expression were induced both in the ventral midbrain as well as in the striatum, and that DA specific loss of p53 diminished MPTP-induced PUMA up-regulation. It is possible that different MPTP injection regimens can lead to distinct apoptotic pathway activations Since the PUMA gene is regulated by multiple cell death pathways, inhibition of PUMA might be more potent in blocking cell death than p53 inhibition. In addition, since inhibition of PUMA does not directly cause spontaneous malignancies, therapeutics to inhibit PUMA might have fewer side effects and be safer for clinical treatment development.

p53 isorforms have been reported since 2005, and have been implicated to play important roles in determining the survival and proliferation of cells when changes in cell homeostasis occurs. It has been reported recently that regulation of alternative splicing of TRP53 gene modifies cellular responses by altering the expression of the p53b or p53g isoforms. It would be interesting to examine the expression profile of different isoforms after MPTP exposure in future studies. Models that could permit the separation of these factors to allow the characterization of p53 actions in neurons are thus important. In our study, the two loxP sites flank exon1-exon10 of the TRP53 gene, leading to complete loss of p53 protein (Jonkers et al. 2001).

In PD patients, increased number of astocytes as well as GFAP expression have been reported (Forno *et al.* 1992, Miklossy *et al.* 2006). Moreover, astrocytic activation has been a key finding after MPTP exposures (O'Callaghan & Jensen 1992, Forno et al. 1992). Studies have suggested that activated glial cells might participate in the propagation of dopaminergic

neuronal death by release of inflammatory cytokines and production of ROS (Cabezas *et al.* 2013, Hirsch*et al.* 2003). We thus examined whether astrocytes are still activated in the absence of dopaminergic neuronal p53 activity and diminished DA neuronal loss. GFAP positive activated astrocytes were found both in striatum and SN in both WT and DA-p53 KO mice. There was no difference in GFAP gene upregulation both in striatum and SN, nor was there any difference in striatal GFAP immunostaining intensity between WT and DA-p53 KO mice. This suggests that, in our acute MPTP model, astrocytic activation might not be directly linked to dopaminergic neuronal death. Although DA-p53 KO mice have diminished DA neuronal loss compared to WT, DA-p53 KO mice still have significant loss of TH fibers in striatum, which might be attributed to astrocyte activation in striatum. Therapeutic strategies that inhibit striatal glisosis might therefore be helpful to prevent DA axonal terminal loss in addition to p53 inhibition.

Taken together, our results show that selective depletion of p53 in dopaminergic neurons inhibited p53 downstream pro-apoptotic genes, increased the survival of dopaminergic neurons in the nigrostriatal system and reduced behavioral motor deficits in our MPTP-induced Parkinsonism mouse model. Our results further support the role of programmed cell death mediated by p53 in this animal model of PD. In contrast, such selective depletion had no effects on the process of normal aging and astrocyte-mediated gliosis. Therefore, the DAT-cre-p53 mouse line might provide a unique tool to study the mechanism of DA neuronal degeneration in PD.

Acknowledgement

This study is supported by NINDS R01NS094152, R01 NS091213, the Spitz Brain Health Innovation Award, MOST 101-2632-B-038-001-MY3 from Taiwan, and by the Intramural Research Program of the National Institute on Aging, NIH. We would like to thank Larimee Cortnik for help in preparation of the manuscript.

List of abbreviations

PD	Parkinson's disease
DA	dopamine
MPTP	1-methyl-4-phenyl-1,2,3,6-tetrahydropyridine
PUMA	*p53* upregulated modulator of apoptosis
SN	Substantia nigra
DAT	Dopamine transporter
KO	Knockout
PTEN	Phosphatase and tensin homolog
NIH	National Institutes of Health
UTR	Untranslated region
IRES	Internal ribosome entry site sequence

TH	tyrosine hydroxylase
PFA	paraformaldehyde
qRT-PCR	Quantitative reverse transcription-PCR
BSA	bovine serum albumin
PB	phosphate buffer
GFAP	Glial fibrillary acidic protein
TBS	Tris-buffered saline
HEPES	4-(2-hydroxyethyl)-1-piperazineethanesulfonic acid
EGTA	ethylene glycol-bis(β-aminoethyl ether)-N,N,N',N'-tetraacetic acid
SDS-PAGE	sodium dodecyl sulfate polyacrylamide gel electrophoresis
ECL	Enhanced Chemiluminescence
VTA	ventral tegmental area
ANOVA	Analysis of variance
ROS	Reactive oxygen species

References

Alves da Costa C, Checler F. Apoptosis in Parkinson's disease: is p53 the missing link between genetic and sporadic Parkinsonism? Cellular signalling. 2011; 23:963–968. [PubMed: 20969953]

Armstrong JF, Kaufman MH, Harrison DJ, Clarke AR. High-frequency developmental abnormalities in p53-deficient mice. Current biology : CB. 1995; 5:931–936. [PubMed: 7583151]

Backman CM, Malik N, Zhang Y, Shan L, Grinberg A, Hoffer BJ, Westphal H, Tomac AC. Characterization of a mouse strain expressing Cre recombinase from the 3' untranslated region of the dopamine transporter locus. Genesis. 2006; 44:383–390. [PubMed: 16865686]

Bernstein AI, O'Malley KL. MPP+-induces PUMA- and p53-dependent, but ATF3-independent cell death. Toxicology letters. 2013; 219:93–98. [PubMed: 23500530]

Blesa J, Phani S, Jackson-Lewis V, Przedborski S. Classic and new animal models of Parkinson's disease. Journal of biomedicine & biotechnology. 2012; 2012:845618. [PubMed: 22536024]

Cabezas R, Avila MF, Torrente D, El-Bachá RS, Morales L, Gonzalez J, Barreto GE. Kishore U. Astrocytes Role in Parkinson: A Double-Edged Sword. Neurodegenerative Diseases. 2013:491–518.

Chipuk JE, Kuwana T, Bouchier-Hayes L, Droin NM, Newmeyer DD, Schuler M, Green DR. Direct activation of Bax by p53 mediates mitochondrial membrane permeabilization and apoptosis. Science. 2004; 303:1010–1014. [PubMed: 14963330]

Culmsee C, Mattson MP. p53 in neuronal apoptosis. Biochemical and biophysical research communications. 2005; 331:761–777. [PubMed: 15865932]

da Costa CA, Sunyach C, Giaime E, et al. Transcriptional repression of p53 by parkin and impairment by mutations associated with autosomal recessive juvenile Parkinson's disease. Nature cell biology. 2009; 11:1370–1375. [PubMed: 19801972]

de la Monte SM, Sohn YK, Ganju N, Wands JR. P53- and CD95-associated apoptosis in neurodegenerative diseases. Laboratory investigation; a journal of technical methods and pathology. 1998; 78:401–411. [PubMed: 9564885]

Diaz-Ruiz O, Zapata A, Shan L, Zhang Y, Tomac AC, Malik N, de la Cruz F, Backman CM. Selective deletion of PTEN in dopamine neurons leads to trophic effects and adaptation of striatal medium spiny projecting neurons. PloS one. 2009; 4:e7027. [PubMed: 19750226]

Donehower LA. The p53-deficient mouse: a model for basic and applied cancer studies. Seminars in cancer biology. 1996; 7:269–278. [PubMed: 9110404]

Duplan E, Giaime E, Viotti J, et al. ER-stress-associated functional link between Parkin and DJ-1 via a transcriptional cascade involving the tumor suppressor p53 and the spliced X-box binding protein XBP-1. Journal of cell science. 2013; 126:2124–2133. [PubMed: 23447676]

Filichia E, Shen H, Zhou X, Qi X, Jin K, Greig N, Hoffer B, Luo Y. Forebrain neuronal specific ablation of p53 gene provides protection in a cortical ischemic stroke model. Neuroscience. 2015; 295:1–10. [PubMed: 25779964]

Forno LS, DeLanney LE, Irwin I, Di Monte D, Langston JW. Astrocytes and Parkinson's disease. Progress in brain research. 1992; 94:429–436. [PubMed: 1287728]

Franklin, KBJ.; P. G.. The mouse brain in stereotaxic coordinates. Academic Press; 1997.

Hartmann A, Michel PP, Troadec JD, Mouatt-Prigent A, Faucheux BA, Ruberg M, Agid Y, Hirsch EC. Is Bax a mitochondrial mediator in apoptotic death of dopaminergic neurons in Parkinson's disease? Journal of neurochemistry. 2001; 76:1785–1793. [PubMed: 11259496]

Hattori T, McGeer PL. Synaptogenesis in the corpus striatum of infant rat. Experimental neurology. 1973; 38:70–79. [PubMed: 4120090]

Hirata H, Cadet JL. p53-knockout mice are protected against the long-term effects of methamphetamine on dopaminergic terminals and cell bodies. Journal of neurochemistry. 1997; 69:780–790. [PubMed: 9231739]

Hirsch EC, Breidert T, Rousselet E, Hunot S, Hartmann A, Michel PP. The role of glial reaction and inflammation in Parkinson's disease. Annals of the New York Academy of Sciences. 2003; 991:214–228. [PubMed: 12846989]

Hutter-Saunders JA, Gendelman HE, Mosley RL. Murine motor and behavior functional evaluations for acute 1-methyl-4-phenyl-1,2,3,6-tetrahydropyridine (MPTP) intoxication. Journal of neuroimmune pharmacology : the official journal of the Society on NeuroImmune Pharmacology. 2012; 7:279–288. [PubMed: 21431472]

Jackson-Lewis V, Vila M, Djaldetti R, Guegan C, Liberatore G, Liu J, O'Malley KL, Burke RE, Przedborski S. Developmental cell death in dopaminergic neurons of the substantia nigra of mice. J Comp Neurol. 2000; 424:476–488. [PubMed: 10906714]

Jin Y, Raviv N, Barnett A, Bambakidis NC, Filichia E, Luo Y. The shh signaling pathway is upregulated in multiple cell types in cortical ischemia and influences the outcome of stroke in an animal model. PloS one. 2015; 10:e0124657. [PubMed: 25927436]

Jonkers J, Meuwissen R, van der Gulden H, Peterse H, van der Valk M, Berns A. Synergistic tumor suppressor activity of BRCA2 and p53 in a conditional mouse model for breast cancer. Nature genetics. 2001; 29:418–425. [PubMed: 11694875]

Kawamata M, Ochiya T. Two distinct knockout approaches highlight a critical role for p53 in rat development. Scientific reports. 2012; 2:945. [PubMed: 23230510]

Kim WR, Sun W. Programmed cell death during postnatal development of the rodent nervous system. Development, growth & differentiation. 2011; 53:225–235.

Langston JW, Forno LS, Tetrud J, Reeves AG, Kaplan JA, Karluk D. Evidence of active nerve cell degeneration in the substantia nigra of humans years after 1-methyl-4-phenyl-1,2,3,6-tetrahydropyridine exposure. Annals of neurology. 1999; 46:598–605. [PubMed: 10514096]

Lee KS, Lee JK, Kim HG, Kim HR. Differential Effects of 1-methyl-4-phenyl-1,2,3,6-tetrahydropyridine on Motor Behavior and Dopamine Levels at Brain Regions in Three Different Mouse Strains. The Korean journal of physiology & pharmacology : official journal of the Korean Physiological Society and the Korean Society of Pharmacology. 2013; 17:89–97.

Liang Y, Liu J, Feng Z. The regulation of cellular metabolism by tumor suppressor p53. Cell & bioscience. 2013; 3:9. [PubMed: 23388203]

Linden R. The survival of developing neurons: a review of afferent control. Neuroscience. 1994; 58:671–682. [PubMed: 8190251]

Luft AR, Buitrago MM. Stages of motor skill learning. Molecular neurobiology. 2005; 32:205–216. [PubMed: 16385137]

Luo Y, Kuo CC, Shen H, Chou J, Greig NH, Hoffer BJ, Wang Y. Delayed treatment with a p53 inhibitor enhances recovery in stroke brain. Annals of neurology. 2009; 65:520–530. [PubMed: 19475672]

Luo Y, Wang Y, Kuang SY, Chiang YH, Hoffer B. Decreased level of Nurr1 in heterozygous young adult mice leads to exacerbated acute and long-term toxicity after repeated methamphetamine exposure. PloS one. 2010; 5:e15193. [PubMed: 21151937]

Miklossy J, Doudet DD, Schwab C, Yu S, McGeer EG, McGeer PL. Role of ICAM-1 in persisting inflammation in Parkinson disease and MPTP monkeys. Experimental neurology. 2006; 197:275–283. [PubMed: 16336966]

Miller RM, Callahan LM, Casaceli C, et al. Dysregulation of gene expression in the 1-methyl-4-phenyl-1,2,3,6-tetrahydropyridine-lesioned mouse substantia nigra. The Journal of neuroscience : the official journal of the Society for Neuroscience. 2004; 24:7445–7454. [PubMed: 15329391]

Miller RM, Chen LL, Kiser GL, Giesler TL, Kaysser-Kranich TM, Palaniappan C, Federoff HJ. Temporal evolution of mouse striatal gene expression following MPTP injury. Neurobiology of aging. 2005; 26:765–775. [PubMed: 15708451]

Mogi M, Kondo T, Mizuno Y, Nagatsu T. p53 protein, interferon-gamma, and NF-kappaB levels are elevated in the parkinsonian brain. Neuroscience letters. 2007; 414:94–97. [PubMed: 17196747]

O'Callaghan JP, Jensen KF. Enhanced expression of glial fibrillary acidic protein and the cupric silver degeneration reaction can be used as sensitive and early indicators of neurotoxicity. Neurotoxicology. 1992; 13:113–122. [PubMed: 1508411]

Perier C, Bove J, Wu DC, et al. Two molecular pathways initiate mitochondria-dependent dopaminergic neurodegeneration in experimental Parkinson's disease. Proceedings of the National Academy of Sciences of the United States of America. 2007; 104:8161–8166. [PubMed: 17483459]

Schumm S, Sebban C, Cohen-Salmon C, et al. Aging of the dopaminergic system and motor behavior in mice intoxicated with the parkinsonian toxin 1-methyl-4-phenyl-1,2,3,6-tetrahydropyridine. Journal of neurochemistry. 2012; 122:1032–1046. [PubMed: 22708926]

Tatton NA. Increased caspase 3 and Bax immunoreactivity accompany nuclear GAPDH translocation and neuronal apoptosis in Parkinson's disease. Experimental neurology. 2000; 166:29–43. [PubMed: 11031081]

Trimmer PA, Smith TS, Jung AB, Bennett JP Jr. Dopamine neurons from transgenic mice with a knockout of the p53 gene resist MPTP neurotoxicity. Neurodegeneration : a journal for neurodegenerative disorders, neuroprotection, and neuroregeneration. 1996; 5:233–239.

Vila M, Jackson-Lewis V, Guegan C, Wu DC, Teismann P, Choi DK, Tieu K, Przedborski S. The role of glial cells in Parkinson's disease. Current opinion in neurology. 2001a; 14:483–489. [PubMed: 11470965]

Vila M, Jackson-Lewis V, Vukosavic S, Djaldetti R, Liberatore G, Offen D, Korsmeyer SJ, Przedborski S. Bax ablation prevents dopaminergic neurodegeneration in the 1-methyl-4-phenyl-1,2,3,6-tetrahydropyridine mouse model of Parkinson's disease. Proceedings of the National Academy of Sciences of the United States of America. 2001b; 98:2837–2842. [PubMed: 11226327]

West MJ, Gundersen HJ. Unbiased stereological estimation of the number of neurons in the human hippocampus. The Journal of comparative neurology. 1990; 296:1–22. [PubMed: 2358525]

Yin HH, Mulcare SP, Hilario MR, Clouse E, Holloway T, Davis MI, Hansson AC, Lovinger DM, Costa RM. Dynamic reorganization of striatal circuits during the acquisition and consolidation of a skill. Nature neuroscience. 2009; 12:333–341. [PubMed: 19198605]

Yokoyama H, Uchida H, Kuroiwa H, Kasahara J, Araki T. Role of glial cells in neurotoxin-induced animal models of Parkinson's disease. Neurological sciences : official journal of the Italian Neurological Society and of the Italian Society of Clinical Neurophysiology. 2011; 32:1–7.

Yokoyama M, Okada S, Nakagomi A, et al. Inhibition of endothelial p53 improves metabolic abnormalities related to dietary obesity. Cell reports. 2014; 7:1691–1703. [PubMed: 24857662]

Zhang Y, Granholm AC, Huh K, et al. PTEN deletion enhances survival, neurite outgrowth and function of dopamine neuron grafts to MitoPark mice. Brain : a journal of neurology. 2012; 135:2736–2749. [PubMed: 22961549]

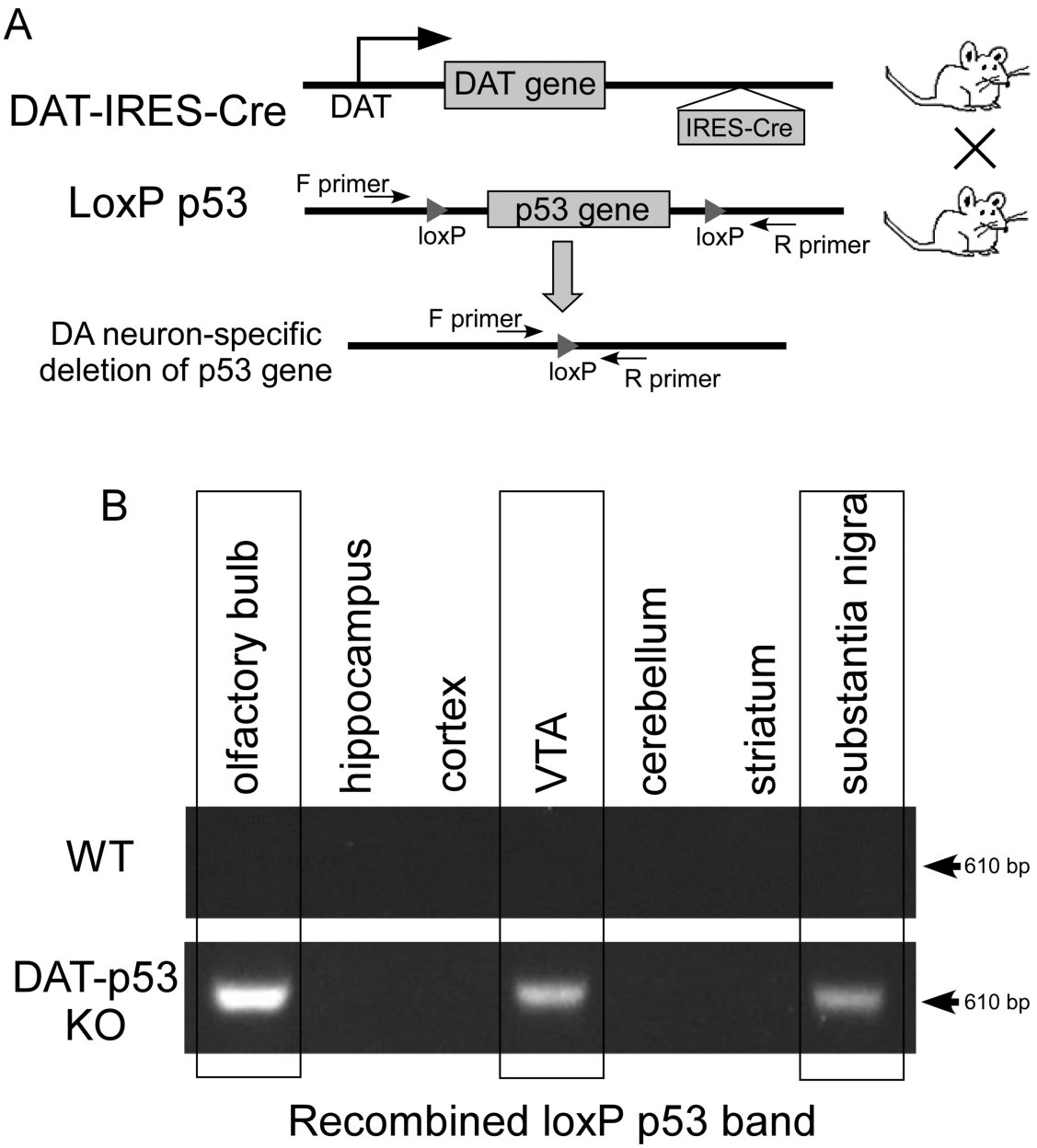

Fig 1.

Generation of dopaminergic neuron-specific p53 KO mice. A. Strategy for dopaminergic neuronal specific deletion of the p53 gene in DAT-p53 KO mice. B. Detection of recombined alleles (indicating deletion of p53 gene) in olfactory bulb, substantia nigra and the ventral tegmental area but not in hippocampus, cortex, cerebellum or striatum of KO mice (upper panel). There is no recombination in different brain areas in WT mice.

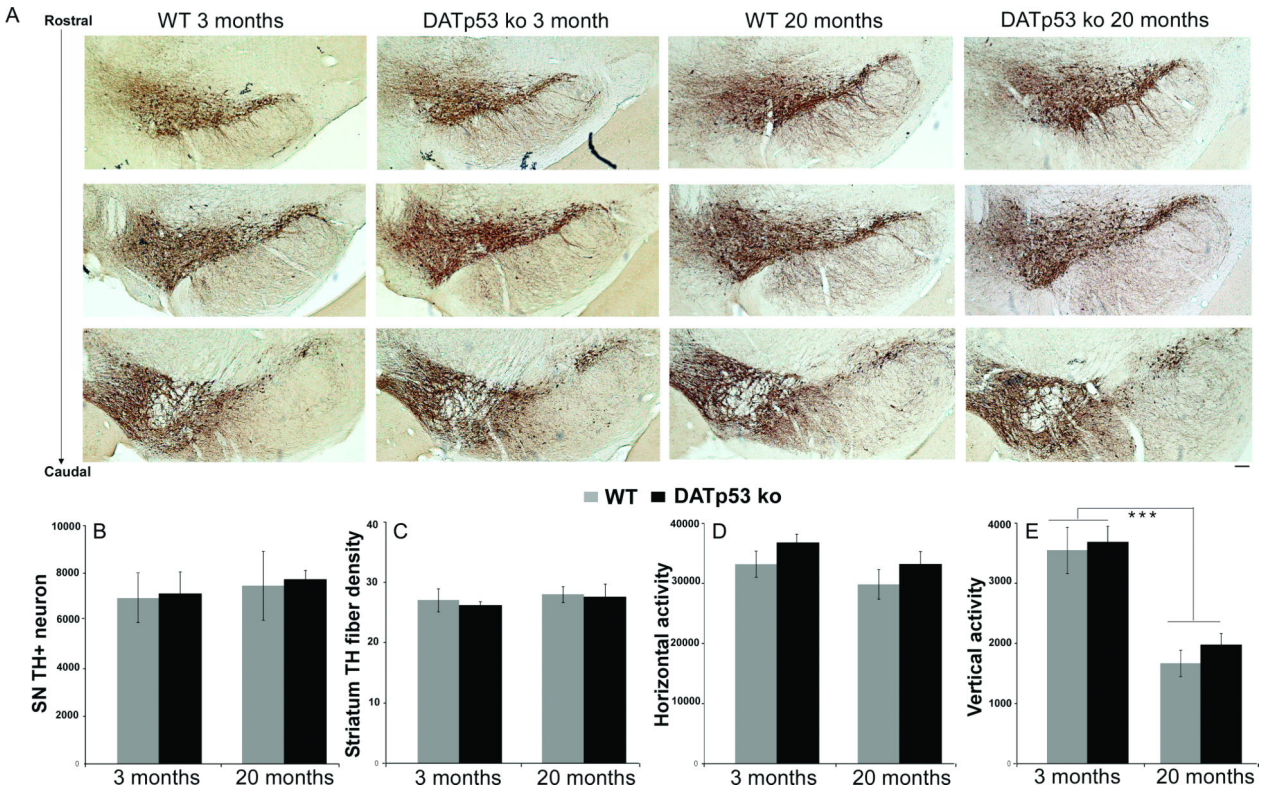

Fig 2.

p53 gene deletion in dopaminergic neurons does not affect development and aging of dopaminergic neurons. Immunohistochemical staining for TH in the ventral midbrain of young (3 month) and old (20 month) WT and DA-p53t KO mice at three different sites ranging from rostral to caudual. (*A*) To determine the effect of p53 ablation on DA neuron survival in young and old mice, we compared the number of TH-positive cells and the regional organization of the ventral midbrain in adult animals. No differences were found in the general morphological appearance between the ventral midbrain in adult WT and KO animals. (*B*) The total number of TH-positive neurons in SN were similar in young and old WT compared to DA-p53 KO mice. Two way ANOVA; $P > 0.05$ for genotypes and age. (C) Total TH immunoreactive fiber density was similar in young and old WT or DA-p53 KO mice. Total spontaneous locomotion activity measured by horizontal activity (D) was similar in young and old WT or in DA-p53 KO mice. Two way ANOVA; $P > 0.05$ for genotypes and age. (E) Total vertical activity is decreased in old mice compared to young mice but there is no difference between genotypes. Data are mean ± SE. *** $P<0.001$ for young vs old, and $P>0.05$ for genotypes, Two way ANOVA. Scale bar =100um.

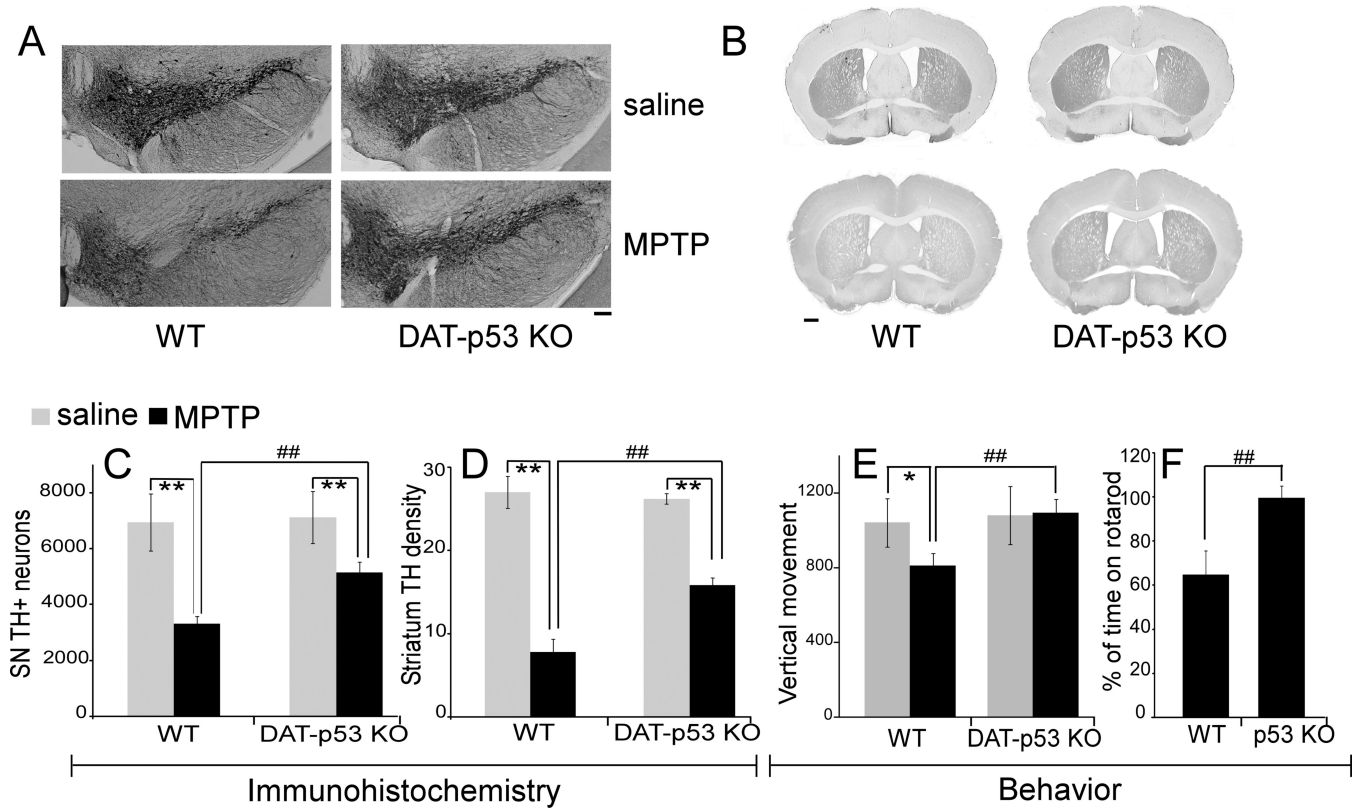

Fig 3.

p53 gene deletion in dopaminergic neurons results in neuroprotection in DA-p53 KO mice in an acute MPTP model. (A). Representative images showing immunohistochemical staining for TH in the ventral midbrain in saline or MPTP treated WT or DA-p53 KO mice at 14 days after the last MPTP or saline injection. (B) Representative images showing TH immunostaining in striatum of WT or DA-p53 KO mice treated with saline or MPTP at 14 days post treatment. DA-p53 KO mice exhibit a significant protection against MPTP-induced SNpc DA cell loss as determined by assessing (C) the total number of SNpc DA neurons and (D) total striatal TH immunoreactive optical density at 14 days after the last MPTP injection (** indicates $p<0.01$ for saline vs. MPTP administration, and ## indicates $p< 0.01$ for WT vs. KO, two way ANOVA, with Newman–Keuls post hoc tests. n=5 for WT or KO saline group and n=9 for WT or KO MPTP challenged group). (E) Reduced vertical activity (rearing) in WT, but not DAT-p53 KO mice after MPTP (* indicates $p<0.05$ for saline vs MPTP in WT and ## indicate $p=0.01$ for WT MPTP vs KO MPTP, n=12 each group). (F) Rotarod tests show the time mice proved capable of remaining on the rod at 7 days post MPTP administration, presented as a percentage in relation to the same individual's time on the rotoarod prior to MPTP challenge, for mice in WT or DA-p53 KO groups. Data are mean ± SE. (## $p<0.01$ Student's t-test, n=10-12 each group). Scale bar = 100 um in Panel A and 500um in Panel B.

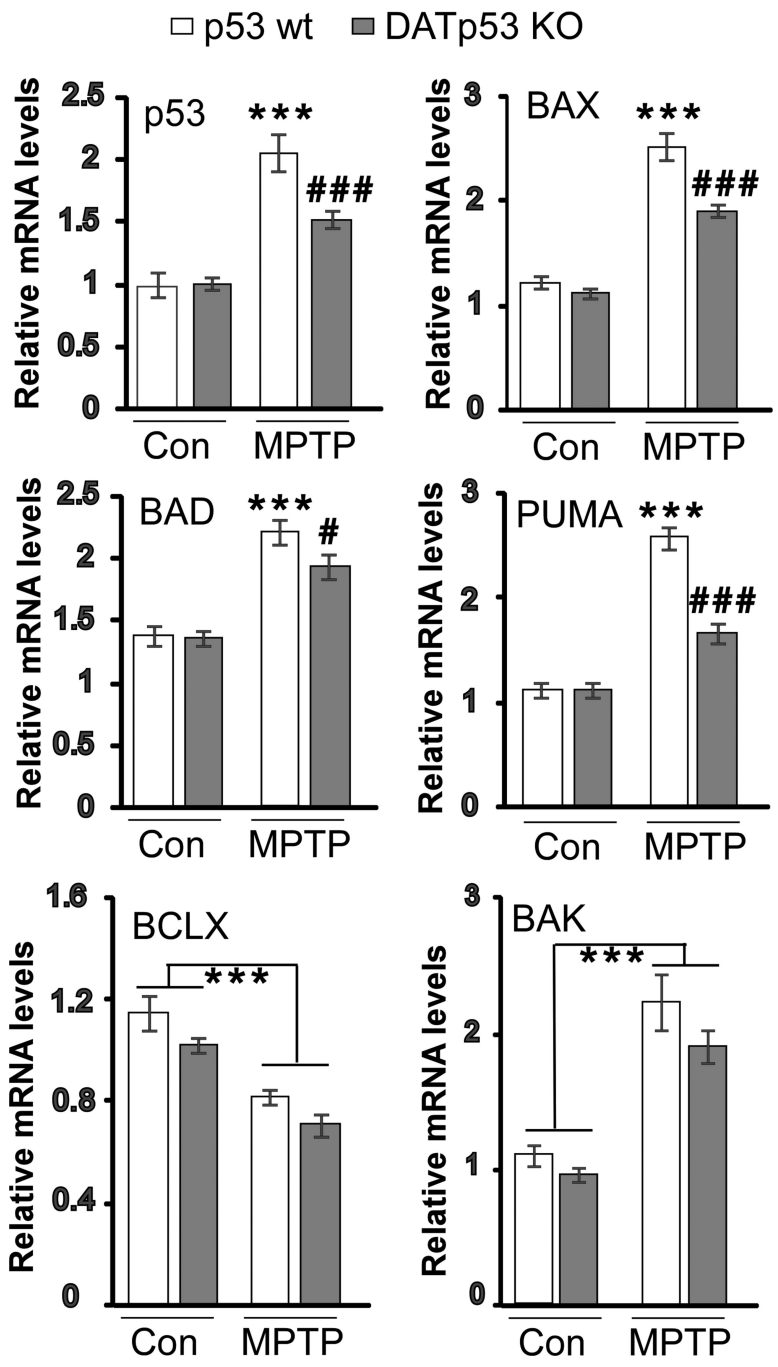

Fig 4.

Dopaminergic neuronal specific p53 deletion results in differential gene transcriptional regulation in the DA system. Brain tissues were harvested after MPTP challenge. qPCR analysis was conducted to determine the expression level of p53 (A), BAX (B), BAD (C), PUMA (D), BCLX (E) and BAK (F) at the indicated groups. Data are shown as mean ± SE. *** p<0.001 WT mice MPTP treated vs saline treated; ### p<0.001 or #<0.05 MPTP treated, KO vs WT. The data was analyzed by two way ANOVA, with Newman–Keuls post hoc tests. n=7-8 each group.

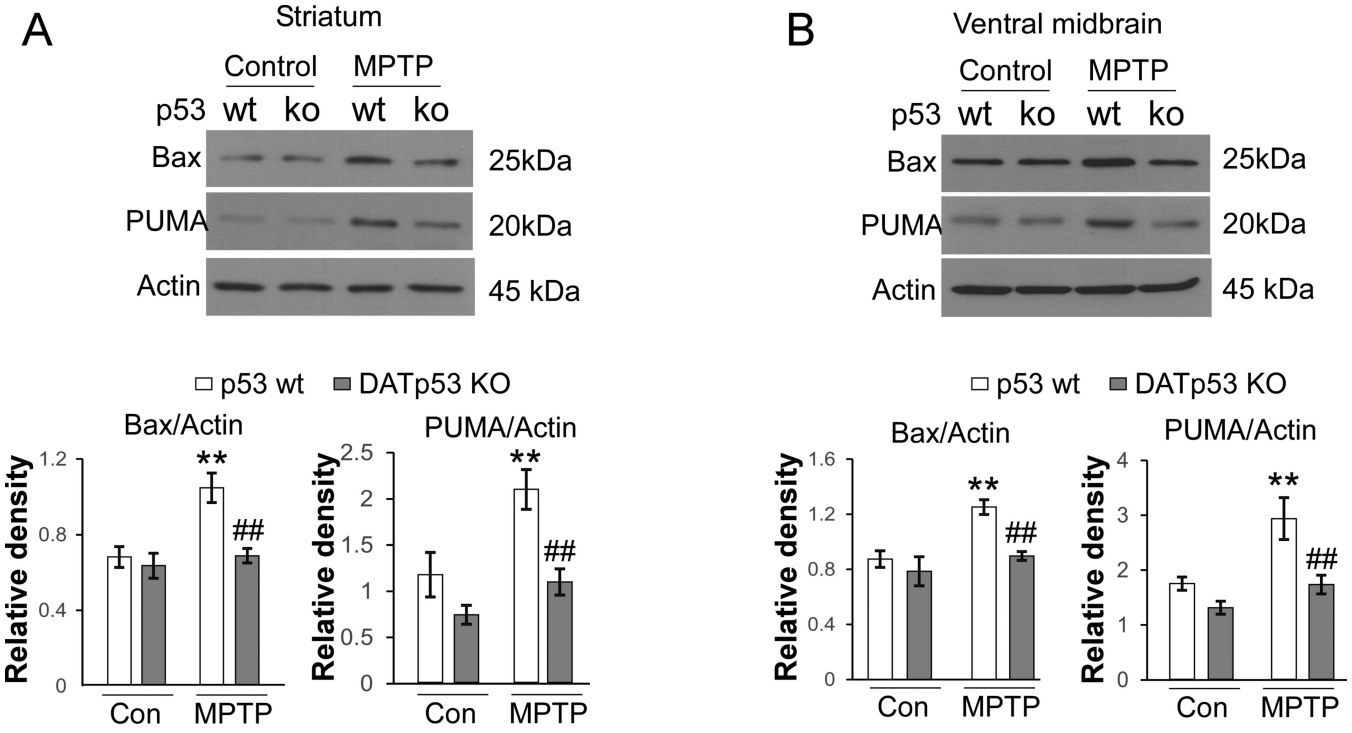

Fig 5.

Dopaminergic neuronal specific p53 deletion in mice inhibits MPTP-induced Bax and PUMA protein upregulation. Brain tissues of striatum and ventral midbrain were harvested at 48 hours after the last MPTP injection. Protein levels of Bax and PUMA both in striatum (A) and ventral midbrain (B) were examined by Western blot analysis. Actin was used as a loading control. Data are mean ± SE. ** $p<0.01$ *vs.* WT mice treated with saline. ## $p<0.01$ vs. WT mice treated with MPTP. The data was analyzed by two-way ANOVA, with Newman–Keuls post hoc tests. n= 4 each group.

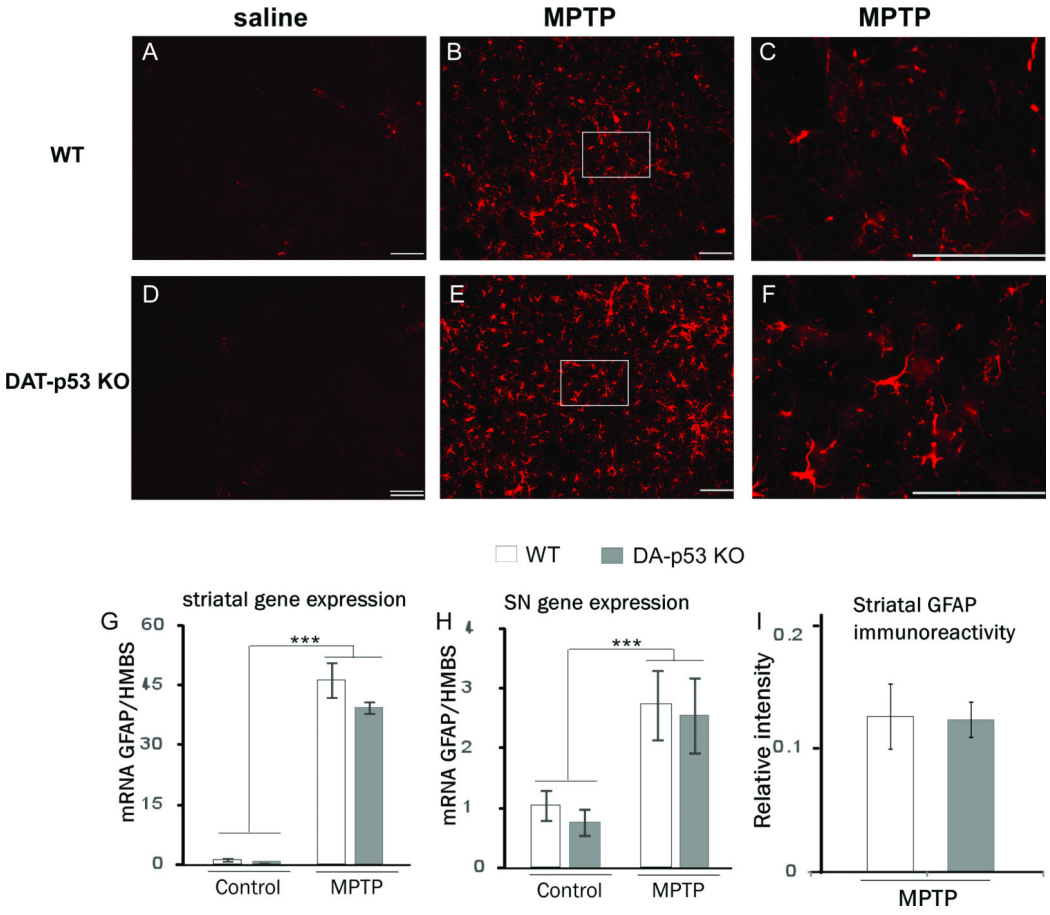

Fig 6.

MPTP-induced astrocyte activation is not altered in DAT-p53 KO mice. Representative images of GFAP immunostaining in striatum in saline injected WT (A) or KO (D) mice showing minimal GFAP positive cells. MPTP injected WT (B) or KO mice (E) indicate significant activation of astocytes as shown by GFAP expression. Right upper and lower panels (C) and (F) are higher magnifications of the framed areas in panels B and E. Scale bar= 100um. GFAP mRNA levels in MPTP injected WT and KO mice are significantly upregulated compared to saline injected WT or KO mice both in striatum (G) and ventral midbrain (H). There is no significant difference between WT and KO mice. ***$p<0.001$ MPTP vs saline, Two way ANOVA, n=7-8 each group (I) Quantification of striatal GFAP immunoreactivity in MPTP injected animals showed no significant difference between WT and KO (n=4 each group). Data are mean ± SE.

Table 1

Primer/ probe sets used in qRT-PCR.

Primer/probe set:		
Hmbs:	Forward Primer:	5′-TCC CTG AAG GAT GTG CCT AC-3′
	Reverse Primer:	5′-ACA AGG GTT TTC CCG TTT G-3′
	Probe:	Universal Probe Library: Probe 79 - Roche
HPRT1:	Forward Primer:	5′-TGA TAG ATC CAT TCC TAT GAC TGT AGA
	Reverse Primer:	5′-AAG ACA TTC TTT CCA GTT AAA GTT GAG
	Probe:	Universal Probe Library: Probe 22 - Roche
p53:	Forward Primer:	5′- GCA ACT ATG GCT TCC ACC TG -3′
	Reverse Primer:	5′- GTA CGT GCA CAT AAC AGA CTT GG -3′
	Probe:	Mouse Universal Probe Library: Probe 4 - Roche
BAX:	Forward Primer:	5′- GTG AGC GGC TGC TTG TCT -3′
	Reverse Primer:	5′- GGT CCC GAA GTA GGA GAG GA -3′
	Probe:	Universal Probe Library: Probe 83 - Roche
PUMA	Forward Primer:	5′- CAT GGG ACT CCT CCC CTT AC -3′
	Reverse Primer:	5′- CAC CTA GTT GGG CTC CAT TT -3′
	Probe:	Universal Probe Library: Probe 1 - Roche
BAD:	Forward Primer:	5′- GGA GCA ACA TTC ATC AGC AG -3′
	Reverse Primer:	5′- TAC GAA CTG TGG CGA CTC C -3′
	Probe:	Universal Probe Library: Probe 83 - Roche
BCLX	Forward Primer:	5′- TGA CCA CCT AGA GCC TTG GA -3′
	Reverse Primer:	5′- TGT TCC CGT AGA GAT CCA CAA -3′
	Probe:	Universal Probe Library: Probe 2 - Roche
BAK:	Forward Primer:	5′- GGA ATG CCT ACG AAC TCT TCA -3′
	Reverse Primer:	5′- CCA GCT GAT GCC ACT CTT AAA -3′
	Probe:	Universal Probe Library: Probe 19 - Roche